

# Solid bonding

Jean-Yves Delenne

*Laboratoire de Mécanique et Génie Civil, CNRS - Université Montpellier 2, Place  
Eugène Bataillon, 34095 Montpellier cedex 05*

## 1 Introduction

The cohesion of granular materials reflects their ability to resist external tensile stresses. This property enhances also the shear strength that is used to assess the cohesion of granular soils from shear tests performed at different confining pressures. The microscopic origin of cohesion is the presence of attraction forces between particles. These interactions, to which we refer as *cohesive interactions*, have different physical and chemical origins. They manifest themselves between two particles by resistance to separation, shear or rolling. The phenomenology of simple interactions can be recovered by integrating the electromagnetic forces acting on very smaller scales. This upscaling procedure is, however, rather complex. Moreover, most properties of granular media emerge from their many-body feature and the dissipative nature of their interactions. For this reason, the relevant scale for modeling granular materials is often that of the particles and the cohesive interactions need to be considered at this scale.

DEM algorithms can easily be extended to account for cohesive interactions which are often simply supplemented to the repulsive elastic and frictional interactions of cohesionless materials. We present here a general framework for the implementation of cohesion in a discrete-element framework. Generally, simple models of interaction laws are privileged in DEM so as to reduce time-consuming operations arising from too many elementary operations. In any case, one has to check the impact of the simplifications on the resulting global behavior of the material.

## 2 Model of contact

In the case of a non-frictional contact, the force acting between two particles is normal to the contact plane and can be additively decomposed into three forces:

$$f_n = f_n^e + f_n^d + f_n^c \quad (1)$$

where  $f_n^e$  is the repulsive force at contact,  $f_n^d$  a viscous force, and  $f_n^c$  the cohesion force.

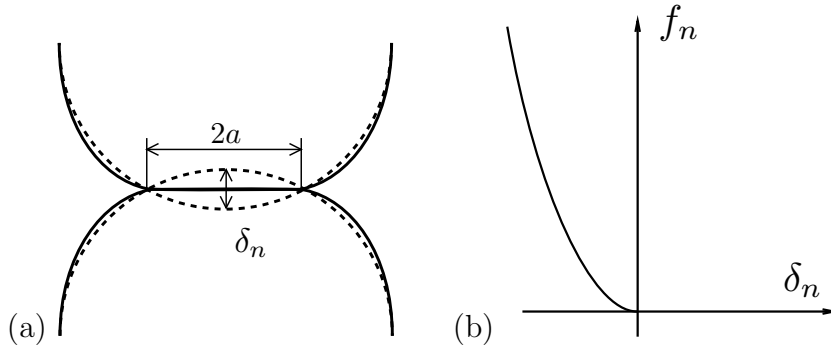


Fig. 1. Hertz contact. (a) Circular contact zone of diameter  $2a$  and contact deflexion  $\delta_n$ . (b) Evolution of the contact force as a function of contact deflexion.

For spherical particles, the contact surface takes the form of a disk of radius  $a$  at which the pressure is not uniformly distributed; figure 1. We make the following assumptions about the contact:

- particles are perfectly smooth;
- the behavior is elastic and isotropic;
- the tangential component of the force does not affect the normal component ;
- the contact deflexion is small ( $\delta_n \ll a$ ).

Under these assumptions, the contact force is given by the Hertz contact law (Maugis [2000]):

$$f_n^e = \frac{4}{3} E^* \sqrt{R^*} (-\delta_n)^{3/2} \quad (2)$$

avec  $\frac{1}{E^*} = \frac{1-\nu_1^2}{E_1} + \frac{1-\nu_2^2}{E_2}$  where  $E_1$  et  $E_2$  are the Young modulus of the two particles and  $\nu_1$  and  $\nu_2$  the poisson ratio and  $R^*$  is the harmonic mean of the particles radii.

For cohesive granular materials, the effect of cohesion often dominates that of confining stresses. The macroscopic behavior is much more dictated by the

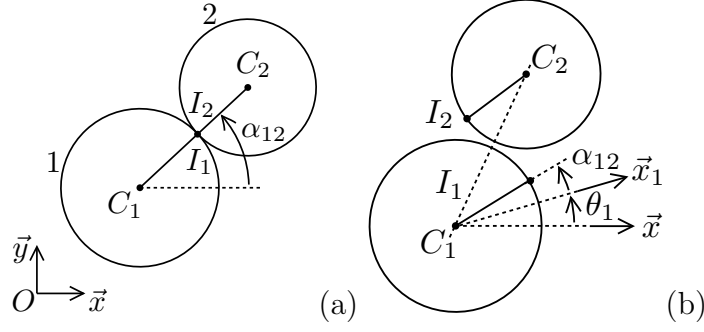


Fig. 2. Kinematic parameters: (a) initial state ( $\theta_1 = 0$ ); (b) deformed state.

cohesive interactions than by the non-linear behavior at the contact. Therefore, a linear approximation of the contact force is relevant:

$$f_n^e = k_n (-\delta_n) \quad (3)$$

where  $k_n$  is the contact normal stiffness.

### 3 Models of cohesive bond

The mechanical approach presented here in a 2D configuration (Delenne et al. [2002]) is a Lagrangian approach where the kinematics and deformations are described from a reference state. The presence of cohesion limits the motion so that the displacements are more relevant than velocity as kinematic variables.

The kinematics is described in a global reference frame  $(O, \vec{x}, \vec{y})$ . We introduce two material points  $I_1$  and  $I_2$  belonging respectively to particle 1 (center  $C_1$  and radius  $R_1$ ) and particle 2 (center  $C_2$  and radius  $R_2$ ); figure 2a and 2b. The reference state is characterized by the coordinates of the centers of particles and their radii. The point of cohesion between two particles 1 and 2 is located by the angle  $\alpha_{12}$ .

At the reference state, the points  $I_1$  and  $I_2$  coincide; figure 2a. Subsequently, these two points are tracked in their movements through the movements and the rotations ( $\theta_1$  and  $\theta_2$ ) of the two particles. The normal  $\delta_n$  and tangential  $\delta_t$  displacements and the rotation  $\theta$  around the cohesion point is calculated in the local frame  $(\vec{n}, \vec{t})$  (where  $\vec{n} = \overrightarrow{C_2C_1} / \|\overrightarrow{C_2C_1}\|$  and  $\vec{t}$  is a unit vector orthogonal to  $\vec{n}$ ):

$$\delta_n = \|\overrightarrow{C_1C_2}\| - (R_1 + R_2) \quad (4)$$

$$\delta_t = \overrightarrow{I_1I_2} \cdot \vec{t} \quad (5)$$

$$\theta = \theta_1 - \theta_2 \quad (6)$$

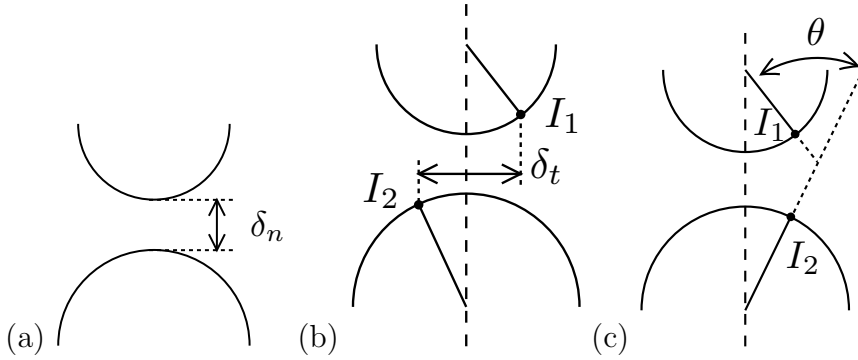


Fig. 3. Degrees of freedom at the local scale (relative displacement at contact): (a) normal displacement  $\delta_n$ ; (b) tangential displacement  $\delta_t$ ; (c) rotation  $\theta$ .

The cohesion is taken into account through local relationships between the displacements  $(\delta_n, \delta_t, \theta)$  and the contact force  $(f_n, f_t, M)$  where  $M$  is the torque at contact. In general, these relationships can be expressed as a cohesion law  $\psi$ :

$$(f_n, f_t, M) = \psi(\delta_n, \delta_t, \theta) \quad (7)$$

A local failure criterion governs the transition between the cohesion state and the sliding-contact state. This criterion is expressed through a yield function:

$$\kappa(f_n, f_t, M)^{rupt} = 0 \quad (8)$$

Different failure criteria may be used depending on the nature of the interface. Figure 4a shows the case of a failure criterion only based on in tensile strength. In this case, we consider that no rupture occurs in pure shear or torsion. This extreme case is similar to the case of normal adhesion for which the action of cohesion is only normal to the contact.

In the case of cemented particles, the failure may occur in tension, but also under shearing and bending. Moreover, for particles that are not in contact because of the presence of an interposed thick binder, fracture may occur in compression. In this case it may be necessary to use different failure thresholds for the different degrees of freedom; figure 4b. It may also be necessary to take into account the cross effects due to combined loading such as compression plus shearing or tension plus torque. This can be done by using more complex criteria of elliptical shape, for example; figure 4c.

To test the relevance of this approach, the cohesion law and failure criteria were determined experimentally for a 2D model material consisting of aluminum cylinders glued together with an epoxy resin (Delenne et al. [2004]). Tensile, compression and shear forces as well as torques were applied on a pair of two cylinders with a cohesive bond. For this model medium, these experiments

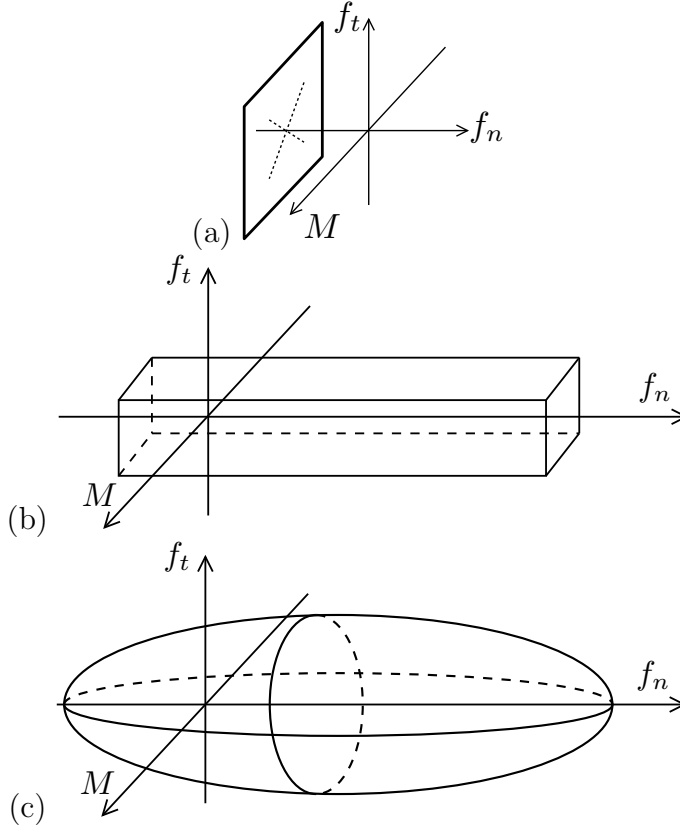


Fig. 4. Example of failure criteria for a cohesive bond.

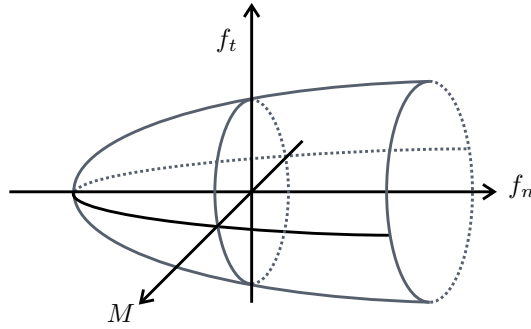


Fig. 5. Failure criterion of paraboloid shape.

show that the compressive failure threshold is very high compared to the threshold in tension so that the threshold in compression may be set to infinity (Figure 5). A paraboloidal yield surface was found to fit the data and used in the numerical simulations:

$$\kappa = \left(\frac{f_t}{f_t^c}\right)^2 + \left(\frac{M}{M^c}\right)^2 + \frac{f_n}{f_n^c} - 1 \quad (9)$$

For  $\kappa < 0$ , there is cohesion bond, otherwise the bond fails and the contact becomes frictional without cohesion. In the case of an irreversible failure (no

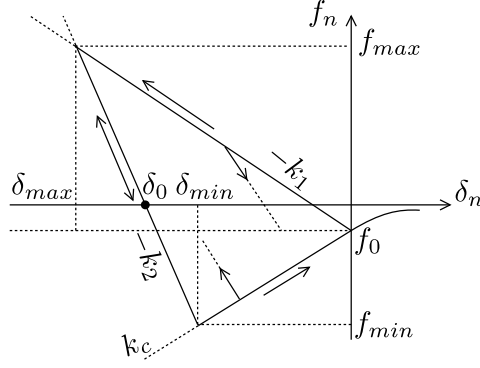


Fig. 6. Adhesion model with hysteresis.

rejoining), one can use a parameter  $\eta$  which describes the damaged state of the bond (Delenne et al. [2008]). Another possibility is to modify the yield surface, corresponding to transition from elastic behavior to plastic behavior with a hardening parameter.

Luding *et al.* proposed a model for plastic contact as shown in figure 6. This model takes into account the normal direction but can easily be extended to more complex loading paths:

$$f^n = \begin{cases} -k_1 \delta_n & \text{si } -k_2 (\delta_n - \delta_0) \geq -k_1 \delta_n \\ -k_2 (\delta_n - \delta_0) & \text{si } -k_1 \delta_n > -k_2 (\delta_n - \delta_0) > k_c \delta_n \\ k_c \delta_n & \text{si } k_c \delta_n \geq -k_2 (\delta_n - \delta_0) \end{cases} \quad (10)$$

where  $k_1 < k_2$ . Note that for an initial load, the force increases linearly with the deflection  $\delta$  to a maximum value  $\delta_{max}$ . The maximum value is stored as a memory variable. The line of slope  $k_1$  is the limit value of force for a given value of  $\delta$ . During unloading, the force declines along the line of slope  $k_2$  down to 0 for values of  $\delta$  which vary from  $\delta_{max}$  to  $\delta_0 = (1 - k_1/k_2) \delta_{max}$ . The value  $\delta_0$  represents a plastic deformation at contact. Upon reloading, the force increases following the line of slope  $k_2$  to the maximum value already reached  $\delta_{max}$  and then follows the line of slope  $k_1$ . Unloading for values below  $f_0$  (defined for  $\delta = \delta_0$ ) leads to an attraction force. This force may decrease until  $f_{min}$  for a value  $\delta_{min} = (k_2 - k_1) \delta_{max} / (k_2 + k_c)$  along the slope  $k_2$ . For  $\delta < \delta_{min}$ , the force follows the slope  $-k_c$ .

## References

- J. Y. Delenne, M. S. El Youssoufi, and J. C. Bénéet. Comportement mécanique et rupture de milieux granulaires cohésifs. *CRAS mécanique*, 330:475–482, 2002.

- Jean-Yves Delenne, Moulay Saïd El Youssoufi, Fabien Cherblanc, and Jean-Claude Benet. Mechanical behaviour and failure of cohesive granular materials. *International Journal for Numerical and Analytical Methods in Geomechanics*, 28(15):1577–1594, 2004. URL <http://dx.doi.org/10.1002/nag.401>.
- J.Y. Delenne, Y. Haddad, J.C. Bénét, and J. Abecassis. Use of mechanics of cohesive granular media for analysis of hardness and vitreousness of wheat endosperm. *Journal of Cereal Science*, 47(3):438–444, 2008.
- D. Maugis. *Contact, Adhesion and Rupture of Elastic Solids*. Springer, 2000.